Systems & Control Transactions

Research Article
Foundations of Computer Aided Process Design (FOCAPD 2024)
Breckenridge, Colorado, USA. July 14-18, 2024
Peer Reviewed Conference Proceeding

PSE PRESS

Integrated Design and Scheduling Optimization of Multi-product processes – case study of Nuclear-Based Hydrogen and Electricity Co-Production

Ruaridh Macdonald[a], Dharik S. Mallapragada[a]*

[a] MIT Energy Initiative, Massachusetts Institute of Technology, Cambridge, MA
* Corresponding Author: dharik@mit.edu

ABSTRACT

Increasing wind and solar electricity generation in power systems increases temporal variability in electricity prices which incentivizes the development of flexible processes for electricity generation and electricity-based fuels/chemicals production. Here, we develop a computational framework for the integrated design and optimization of multi-product processes interacting with the grid under time-varying electricity prices. Our analysis focuses on the case study of nuclear-based hydrogen (H_2) and electricity generation, involving nuclear power plants (NPP) producing high temperature heat and electricity coupled with a high temperature steam electrolyzers (HTSE) for H_2 production. The ability to co-produce H_2 along with nuclear is widely seen as critical to improving the economics of nuclear energy technologies. To that end, our model focuses on evaluating the least-cost design and operations of the NPP-HTSE system while accounting for: a) power consumption variation with current density for the HTSE and the associated capital and operating cost trade-off, b) heat integration between NPP and HTSE and c) temporal variability in electricity prices and their impact on plant operations to meet a baseload hydrogen demand. Instead of formulating a monolithic optimization model, which would be computationally expensive, we propose a decomposition approach that reformulates the original problem into three sub-problems solved in an iterative manner to find near-optimal solutions. Through a numerical case study, we demonstrate the potential synergies of NPP and HTSE integration under alternative electricity price scenarios. This synergy is measured via the metric of relative breakeven H_2 selling price that accounts for the opportunity cost of reduced electricity sales from H_2 co-production.

Keywords: Hydrogen, Nuclear, Multiscale Modelling, Energy Systems, Electricity & Electrical Devices,

INTRODUCTION

Despite its significant share of generation today and importance for climate change mitigation, nuclear power faces economic hurdles in many U.S. and other regions primarily due to depressed wholesale electricity prices stemming from increasing electricity generation from natural gas and variable renewable energy (VRE). For instance, between 2013 and 2021, 9.4 GW of existing nuclear power plants (NPP) have retired in the U.S. with an additional 7.2 GW scheduled to retire by 2025, mostly in regions with restructured electricity markets [1]. This economic outlook for existing U.S. NPPs also makes investments in new NPPs, based on next-gen small modular reactor (SMR) concepts, challenging. However, despite their higher capital costs per kW relative to VRE generation sources, these NPP designs represent a type of low-carbon, dispatchable generation resource which has been shown to be critical to minimizing the cost of achieving deeply decarbonized power systems [2]. NPPs are not fully compensated for this benefit in current markets, so there is a need for alternative business models and revenue streams to support deployment of new NPPs to support economy-wide decarbonization goals.

In this context, the ability to deploy NPPs for simultaneously co-producing low-carbon hydrogen (H_2) via water electrolysis that can be used for industrial applications is appealing for several reasons. First, industrial H_2

demand, amounting to ~10 million tonnes per year in the U.S. in 2015 [3], tends to be centralized and constant in its consumption, both of which match well with least-cost NPP designs that tend to favor continuous operation and large-scale deployment. Second, H_2 demand is anticipated to grow, by up to 7X per one estimate [3], as part of efforts to decarbonize difficult to electrify end-uses. Third, high temperature heat available from next-generation nuclear reactors can be used to improve the electrical efficiency of H_2 production (and by extension, other industrial processes) by carrying it out at higher-than-ambient temperatures, such as high temperature steam electrolysis (HTSE) [4].

The design of integrated NPP-HTSE systems to co-produce H_2 and electricity needs to consider: a) the temporal dynamics in the economic value of electricity and its impact on co-product hydrogen price, b) the heterogeneity in design of new NPPs, particularly in terms of the maximum temperature of heat supply, c) the design of heat integration schemes between NPP and HTSE systems and d) the operating performance of the HTSE system, particularly the current density-dependent efficiency and heat management.

Previous NPP-HTSE system analyses have generally focused on light-water or pressurized water NPPs with lower temperatures of heat generation supply [5-7]. These analyses address detailed assessment of plant-level dynamics operations [5] as well as overall economic optimization using less-detailed plant-level models and soft-linking plant and grid-centric models [6-7].

Here, we develop an integrated design and scheduling optimization framework to address co-production of electricity and H_2 under time-varying electricity prices. For a given NPP design, electricity price series and exogeneous H_2 demand, the model can evaluate the cost-effective sizing of HTSE, on-site H_2 storage and other auxiliary units (e.g. heat exchangers) as well as operation over a representative year, while adhering to a range of operational constraints. Crucially, we account for energetic and economic impacts of HTSE operation across a range of current densities & NPP-HTSE heat integrations.

Solving the proposed model in its original form takes several hours, even for representative periods as short as 12 hours. To include much longer representative periods, up to a year at hourly resolution, we accelerate solution of the proposed model by applying a decomposition strategy. This involves iteratively solving an upper-level investment problem sizing the HTSE using a line search algorithm, mid-level problem to size the heat exchanger network, and a lower-level operational model with fixed HTSE and heat exchangers which is formulated as a mixed integer linear program (MILP) and solved via Gurobi [19]. In addition, we utilize a Taylor expansion-based approximation of bilinear terms to speed up computation of the middle and lower-level operational model.

Finally, we propose a new metric of relative break-even price for H_2 production, which as opposed to the levelized cost of hydrogen (LCOH), accounts for the opportunity costs of forgoing electricity outputs in favor of H_2. While the analytical framework has been developed for NPP-HTSE systems, it can be applied to other processes involving multiple co-products and dynamic interaction with the grid (e.g. electrified chemical production).

As a case study, we evaluate the integration of a high-temperature gas cooled reactor (HTGR) based NPP (750 °C) with an HTSE operating at 750 °C, where we quantify the value of heat integration between HTSE and NPP on the cost of hydrogen produced. We test the economics of the proposed system under current-day and future electricity prices and show how the relative break-even price as opposed to the LCOH is the appropriate metric for such multi-product systems.

METHODOLOGY

Process description

Figure 1 shows the schematic for the process where the HTGR is the primary heat source for the power generation and electrolysis processes. The HTGR produces hot gas leaving the reactor at 750 °C that is fed to steam generator producing steam at 565 °C and 16.5 MPa, that is used for power generation via a Rankine cycle [8]. A similar concept was chosen for a pilot project to provide heat and power for a U.S. petrochemical facility [9]. Part of the heat available from the HTGR can be used to improve the energy efficiency of HTSE H_2 production through feed heating. As seen in Figure 1, we allow for reactor to provide high temperature heat for steam superheating and low temperature heat for steam generation.

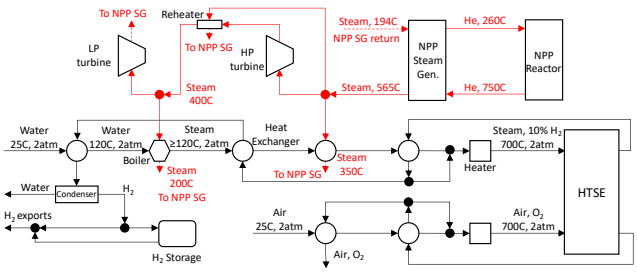

Figure 1. Overview of a high-temperature gas cooled reactor (HTGR) NPP integrated with HTSE operating at 750 °C. The black arrows relate to the HTSE flows and the red lines the nuclear power plant (NPP) flows. For simplicity, we have not shown the return of some steam flows back to the NPP steam generator (SG). All of the temperature and mass flow rates are free variables unless a value is given. The HTSE operating temperature is assumed constant and equal to the feed. Temperature of exhaust streams from HTSE are model variables but

must be within 100 °C of the inlet temperature to avoid thermal gradients [14].

HTSE modeling

A key goal of our analysis was to understand how NPP and HTSEs might vary their electricity and H_2 outputs in response to electricity prices to maximize their profit. Therefore, it was important that we accurately model the dynamic operation of HTSE and how the efficiency varies as a function of the current density.

We developed a 0-D HTSE model based off the generic electrolyzer model produced by Orella [10] along with overpotential calculations from Buttler et al. [11]. The HTSE potential *(V)* as function of current density *(j)* at each time-step is calculated as sum of thermodynamic potential (V_{th}, Eq. 2), ohmic overpotential (V_{ohm}, Eq. 3), concentration overpotential (V_{conc}, Eq. 4-5), and activation overpotential for each electrode ($V_{act,k}$, Eq. 6). Each of these terms are related to SOEC system parameters, such as cell temperature (T), exchange current density ($j_{exchange,k}$), and partial pressures of components. Full details of the terms are given in [11].

$$V = V_{th} + V_{ohm} + V_{conc} + V_{act,c} + V_{act,a} \quad (1)$$

$$V_{th} = V_0 + \frac{RT}{2F}\ln\left(\frac{p_{o2}^{0.5} p_{h2}}{p_{steam}}\right) \quad (2)$$

$$V_{ohm} = -2.99 \times 10^{-5} j \delta e^{-\frac{10300}{T}} \quad (3)$$

$$c = -\frac{100\sqrt{2} j R T t_{cath}}{2FPD_{steam}} \quad (4)$$

$$V_{conc} = \frac{RT}{2F}\ln\left(\frac{1+\frac{c}{f_{h2}}}{1-\frac{c}{f_{steam}}}\right) \quad (5)$$

$$V_{act,k} = \frac{RT}{F}\sinh^{-1}\left(\frac{j}{2j_{exchange,k}}\right) \forall k = a, c \quad (6)$$

Given the HTSE stack area (A) and time-dependent current density j_t (which is linearly proportional to the H_2 production rate for a given HTSE area by Faraday's Law), the power required to operate the HTSE at each time step t is given by Eq. 7, where the cell voltage (V_t) is calculated as per Eq. 1-6 for the given current density.

$$P(j, A, t) = j_t A V_t(j_t) \quad (7)$$

As shown in Fig. 2A, the power consumption per unit HTSE area varies quadratically with the current density, meaning that the electrolyzer energy efficiency decreases with increasing current density owing to greater overpotentials. This creates an incentive to oversize the electrolyzer relative to demand, increasing the electrolyzer area (A) and CAPEX to reduce the current density and hence power consumption required to achieve a given hydrogen production rate. Our modelling results exhibit this CAPEX - OPEX trade-off as we include a piece-wise approximation of the power vs. H_2 production curve for a fixed HTSE area.

The energy balance around the HTSE system is modeled with the constraint that feed stream and HTSE operating temperature are fixed at 750 °C, and the ratio of hydrogen to steam at the cathode is held constant. At each time step, the heat balance of the HTSE is determined by the difference between its electric power demand and the enthalpy of the water splitting reaction, with high (low) current density operation generally leading to greater (less) overpotentials and heat generation. The HTSE is endothermic when operated below the thermoneutral potential (V_{th}). The deficit or excess heat in the HTSE is balanced by either cooling or heating, respectively, the outlet streams. Outlet stream temperatures are model operational variables along with the HTSE stack current density. In this way, the HTSE dynamic operation is coupled with the operation of the heat exchanger network associated with feed preheating and product cooling shown in Fig. 1.

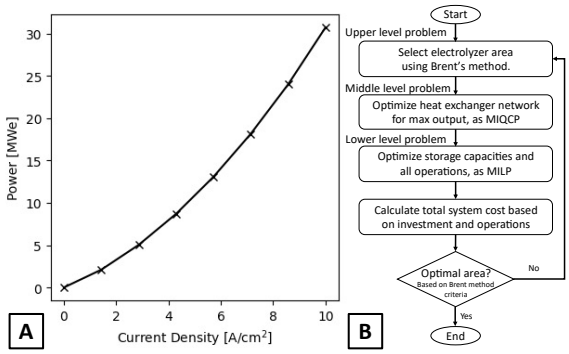

Figure 2. A: example piecewise power – current density relationship used in the model, for a 100m² HTSE producing up to 0.36 tonne H_2 per hour. We used 5 elements in our piecewise approximation. B: Overview of the three-part solution strategy used to optimize our model. MIQCP= Mixed integer quadratically constrained programme. MILP = Mixed linteger linear programme.

Model description and solution strategy

As shown in Eq. 8, the overall problem can be defined as a single mixed integer nonlinear program (MINLP). The objective function of this model is to minimize the total system cost while meeting a constant hourly hydrogen demand and several other operational and capacity constraints associated with units in Fig. 1.

$$\min_{x,y,z} c_1 x + c_2^T \boldsymbol{y} + c_3^T \boldsymbol{z}$$

$$\text{s.t } f(x, y, z) = 0$$

$$h(x, y, z) \leq 0$$

$$g(x, y) \leq 0$$

$$x, y, z \geq 0 \quad (8)$$

In Eq. 8, x is the stack area of the HTSE, $\boldsymbol{y}$ represents the vector of variables corresponding to the areas of the heat exchangers and boilers in the heat exchanger

network, and $\boldsymbol{z}$ is the vector of variables corresponding to the capacity of the electricity and H_2 storage as well as the scheduling decisions for the entire system. Note that $\boldsymbol{z}$ includes both continuous and binary variables, where the latter are associated with NPP start-up/shutdown [8].

Since we are interested in accounting for plant operational dynamics subject to hourly changes in electricity price over the year, solving the monolithic model of Eq. 8 becomes computationally challenging for representative periods longer than 12 hours. Therefore, we decomposed the original problem into three sub-problems that are iteratively solved to find the optimal solution. Fig. 2B shows the sequence of operations, where: a) the upper-level problem sizes the HTSE area, b) the middle-level problem sizes the heat exchanger network for a given HTSE area and maximum H_2 output for HTSE and c) lower-level operational problem evaluates cost-optimal plant operation over the entire year and sizes on-site H_2 storage capacity for a given HTSE area and heat exchanger network (via part a and b).

The upper-level investment problem is solved using Brent's method [12] to search for the HTSE area which minimizes the total system cost (capex + opex, Eq. 8). Brent's method is a gradient-free 1D minima-finding algorithm which combines the inverse quadratic interpolation, secant method, and bisection method. At each iteration, the ordering and value of function evaluations of the previous iterates, i.e. the results of solving the intermediate the lower problems, are compared to select the best methods to calculate the next iterate.

The middle-level problem optimizes the design of the heat exchanger network for a given HTSE area and several operating state of the system, corresponding to zero H_2 output, the mean output, and the maximum H_2 output. The only non-quadratic nonlinear constraints in the model pertain to the logarithmic mean temperature difference (ΔT_{LMTD}) in the heat exchanger sizing constraint. We approximate this by its first order Taylor expansion around initial guesses of the temperature differences ($\Delta_{a,0}, \Delta_{b,0}$) for the various streams, as shown in Eq. 9. We set upper and lower bounds on each stream temperature based on the known temperatures (e.g. the HTSE operating temperature) and used the mid-point of these ranges as the initial temperature guesses.

$$\Delta_a = \left(T_{h,in} - T_{c,out}\right),\ \Delta_b = \left(T_{h,out} - T_{c,in}\right) \quad (9)$$

$$\Delta T_{LMTD} = \frac{\Delta_a - \Delta_b}{\ln(\Delta_a/\Delta_b)} \quad (10)$$

$$\Delta T_{LMTD} \approx \frac{\Delta_{a,0}-\Delta_{b,0}}{\ln(\Delta_{a,0}/\Delta_{b,0})} + \sum_{q\in[(h,in),(c,in)]} \frac{(T_q - T_{q,0})}{\ln(\Delta_{a,0}/\Delta_{b,0})^2}\left(\frac{\Delta_{b,0}-\Delta_{a,0}}{\Delta_{a,0}} \pm \ln\frac{\Delta_{a,0}}{\Delta_{b,0}}\right) + \sum_{q\in[(h,out),(c,out)]} \frac{(T_q - T_{q,0})}{\ln(\Delta_{a,0}/\Delta_{b,0})^2}\left(\frac{\Delta_{a,0}-\Delta_{b,0}}{\Delta_{b,0}} \pm \ln\frac{\Delta_{a,0}}{\Delta_{b,0}}\right) \quad (11)$$

This approximation is correct to within a few percent for the temperature ranges in our problem and is more accurate than using the arithmetic mean of the temperature differences when calculating heat fluxes. We determined the heat exchanger areas by solving this middle-level problem for one hour of operation assuming the HTSE is operating at its mean hydrogen output for the given HTSE area. This problem is small, consisting of approximately 100 variables and 100 constraints with 27 quadratic constraints, and thus can be solved in under a second using Gurobi 10.0.

The lower-level problem is a mixed-integer quadratically constrained program (MIQCP) which optimizes the capacities of the battery and H_2 storage as well as the operating decisions of all the components for each of the 8760 hours of the year. The role of the H_2 storage is to allow for flexible operation of HTSE while meeting baseload H_2 demand. The battery storage could allow for enhancing flexibility of NPP by storing electricity at times of low electricity prices and discharging to operate HTSE or export to grid during high price periods.

To speed up solution of lower-level problem, we make two further approximations to convert it to a mixed-integer linear program (MILP): a) we approximate the HTSE power demand as a 1D piece-wise linear function of the current density using SOS2 constraints (Fig. 2A). b) the remaining quadratic constraints are related to the energy and mass balances in the heat exchanger network and splitters/mixers, respectively. For the bilinear terms, we employed a Taylor expansion-based linearization approach per Eq. 12, similar to the approach undertaken to approximate the LMTD in the middle-level problem.

$$\mathrm{xy} \approx \mathrm{x}_0 y_0 + (x - x_0)y_0 + (y - y_0)x_0 \quad (12)$$

We use the temperatures and mass flow rates from the intermediate problem solution to set x_0 and y_0 . The resulting MILP for a full year at hourly resolution has approximately 400,000 constraints and 400,000 variables and 1.5M non-zero terms after presolve. The solution time typically requires less than 30 seconds to solve the root relaxation followed by about three hours for branch and bound using 16 cores and Gurobi 10.0. The overall solution procedure of Fig. 2B typically requires 8-10 iterations to converge to the cost-optimal investment and operation so the total run time for the overall optimization is approximately 24 hours.

Our decomposition method can be improved in several ways. The upper problem could be solved using a gradient-based solver, making use of the duals of the lower problem. We could also solve more states of the system in the intermediate problem to both find Taylor expansion values for each time step, improving the accuracy of the linearization of the lower problem, and creating a warm start for the lower problem. This would reduce the time required for the branch and bound step.

Case study

We model the co-production of electricity and H_2 via the process in Figure 1 with a NPP with thermal capacity

200 MW_t (80 MW_e), located in Waterford, LA, USA. This location has an existing NPP and is close to many existing H_2 consumers (e.g. petrochemical plants). We assume the plant being optimized must supply a constant H_2 demand of 20 tonne/day, simulating H_2 demand from an industrial user. This means our optimization does not depend on the price of hydrogen. We do not consider cases where a facility can maximize revenue by freely choosing between selling electricity and hydrogen as this would require hourly timeseries of hydrogen prices.

Electricity price scenarios

We evaluate the model outcomes for current grid conditions, represented by 2018 wholesale electricity prices at the Waterford site, as well as future grid scenarios for 2030 and 2050 by NREL for the same region [13]. Figure 3 shows the hourly electricity price distribution of the three price timeseries. The median 2030 price is greater than in 2050 but the distribution has shorter high and low tails. The mean and median 2050 prices are lower than both 2018 and 2030 and there are around 250 hours where electricity is priced at $0/MWh.

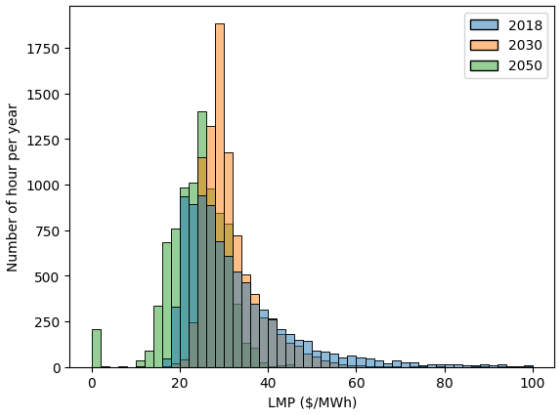

Figure 3. Hourly electricity price distribution for the 3 scenarios evaluted in the study. 2018 prices are realized prices at the Waterford, LA node, while 2030 and 2050 scenarios are sourced from NREL ReEDS capacity expansion model outcomes [13]. Median prices for 2018, 2030 and 2050 are 29, 30, and 25 $/MWh [13,24].

Technology cost and performance assumptions

The major cost and performance assumptions used in the study are summarized in Table 1. We trial cases with and without a $10/MWh transmission charges applied to imports. This charge reflects the difference in wholesale and industrial electricity prices [18].

Relative breakeven price

We evaluated the cost benefits of co-producing electricity and H_2 by comparing the minimum selling price of H_2 produced by a NPP-HTSE co-production facility with the minimum selling price for a standalone HTSE using grid electricity. The minimum H_2 selling price for a standalone HTSE is the price at which the project net present value is zero, i.e. annualized costs are equal to annualized revenues. This is the LCOH of the facility. However, computing the minimum H_2 selling price for a facility selling electricity and H_2 is more complicated since producing H_2 entails not selling the electricity used to produce the H_2. This creates an opportunity cost which must also be recovered in the minimum selling price of the H_2. We call this the relative breakeven price for H_2 associated with a co-production facility.

Table 1. Key cost and performance assumptions

Property	Value	Property	Value
System		**HTSE** [10, 11,15, 16]	
Hourly demand (tonne/hour)	0.83	Fixed costs ($/m^2/yr)	3,770
Discount rate	10%	Temperature (C)	750
NPP [8, 17, 20, 21]		Pressure (atm)	2
Reactor capacity (MWt)	200	Max. current density (A/cm^2)	1
Turbine capacity (MWe)	80	H_2 mole fraction	0.1
CAPEX ($/MWe/yr)	300,000	O_2 mole fraction	0.21
Fixed costs ($/MWe/yr)	71,000	Cathode thickness (μm)	12.5
Variable Cost ($/MWhe)	15	Anode thickness (μm)	17.5
Minimum load	50%	Cell gap (μm)	12.5
Shutdown period (hours)	24	Diffusion coefficient (cm^{-2}s^{-1})	5x10-9
H_2 storage [22]		**Battery** [23]	
Fixed costs ($/MWe/yr)	44,987	Fixed costs ($/MWe/yr)	258,277
Compression energy (kWhe/kg)	0.4	Duration (hours)	4

The relative breakeven price is calculated by finding the H_2 price which ensures a co-production facility earns at least as much profit as the NPP would make if operating independently and only sold electricity. This is done by solving the model in Eq. 8 twice: once as described for the full co-production facility and a second time where x == 0 (i.e. without a HTSE) and the exogenous hydrogen demand is set to zero. In the latter case, the NPP will operate independently selling electricity.

RESULTS

Base system design and operation results

Figure 4A shows the optimal dispatch of the base case system over two weeks using 2018 electricity prices. Given the high cost of HTSEs (Table 1), it is not

Figure 4: Optimal dispatch of NPP and HTSE over two weeks of operation for the 2018 and 2050 electricity price scenario and assumptions summarized in Table 1. Left panel shows reactor thermal balance (left axis) overlaid with electricity price profile right axis, black line) for 2018 while right panel shows results for 2050. In all cases, system meets 20 tonne/day of baseload H_2 demand while adjusting grid electricity exports depending on electricity prices.

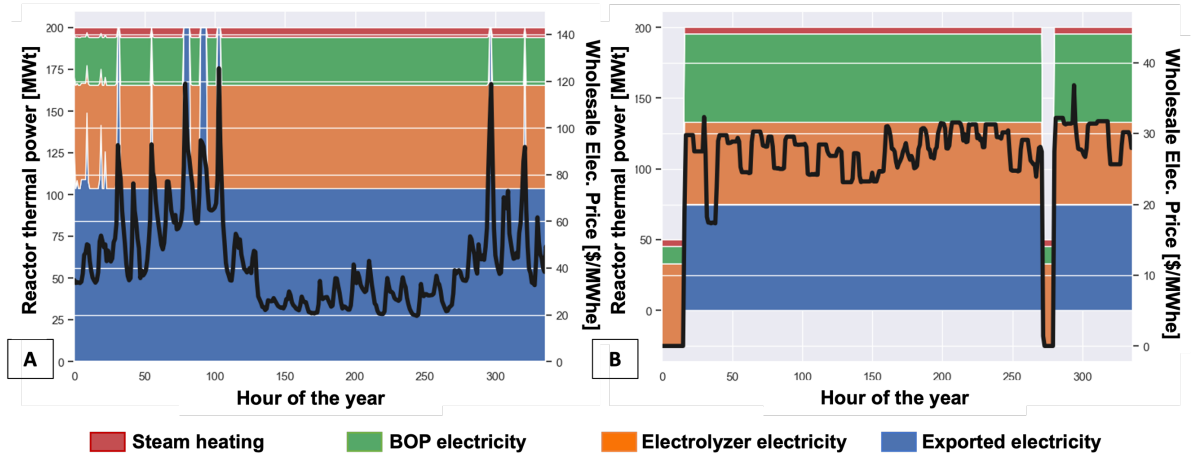

surprising to see that HTSE utilization is quite high despite fluctuating electricity prices. The HTSE output is only reduced during periods of very high electricity prices, when it is more profitable to reduce H_2 production and maximize power exports to the grid. This is enabled by 3 hours of H_2 storage and the HTSE being 8% oversized relative to the minimum HTSE area required to meet the H_2 demand constraint.

It might be expected that the facility would export less power during periods of high prices and use the cheaper electricity generated by the on-site NPP to reduce its average cost of electricity. However, deferring H_2 production till grid prices fall is less expensive overall – as long as storage is cheap enough – because less valuable electricity is used to produce H_2, reducing the opportunity cost of hydrogen production.

The relative breakeven price of the co-produced H_2 accounts for the opportunity cost of lost electricity sales and should be compared to the LCOH of the independent HTSE. These figures are shown in Table 2. In this instance, an independent NPP will be loss-making so the opportunity cost of lost electricity sales is negative. This makes the relative breakeven price of NPP-HTSE H_2 less than its LCOH. An existing co-production facility should be willing to offer H_2 at the relative breakeven price, even though it will lose money on each kilo of H_2, because it will lose less money than if it sold the same electricity.

Clearly, more revenue must be found to make the NPP-HTSE facility profitable overall especially for new facilities. One option is to sell H_2 priced at the LCOH of the NPP-HTSE facility. However, the losses being covered are from the electricity-side of the co-production facility. The relative breakeven price is the price required for the H_2-side of the co-production facility to be profitable. In a scenario with profitable independent NPPs, the relative breakeven price of NPP-HTSE H_2 is higher than its LCOH as the H_2 revenue must also recover the lost NPP profit.

The technical synergies from using NPP heat in the HTSE system reduces the cost of H_2 by approximately $1/kg. We know this because the relative breakeven price of an NPP-HTSE which only exchanges electricity and where no import tariffs were in place should equal the LCOH of an independent HTSE in the same scenario. When there is no asymmetry in the price of buying and selling electricity, the cost of electricity from an onsite NPP is the same as that of purchasing grid power if the opportunity costs of lost NPP sales are also accounted for in the H_2 price. The results in Table 2 show that this is not the case. The relative breakeven price of the NPP-HTSE is $1/kg cheaper than the no-tariff LCOH of the independent electrolyzer, indicating savings from using nuclear heat. This heating is used 5:1 to boil water versus superheat it. This could also be done using low-temperature NPPs, which operate at ~300 C.

H_2 produced by NPP-HTSEs is competitive with that from an independent HTSE, particularly if the grid has import tariffs. However, H_2 produced by both facilities is expensive, especially compared to the $1/kg target. This is due to the relatively high capex of HTSE vs. state-of-art proton exchange membrane (PEM) electrolyzers. In addition, while HTSEs require less electricity input per kg of H2 vs. PEM, they have lower current density limits than PEM electrolysers, typically 1A/cm^2 vs. 2-3A/cm^2. This means a large HTSE is required for the same H_2 output, compounding the cost difference.

Impact of varying electricity price scenarios

Fig. 4B shows the optimal dispatch of the co-

production facility over two weeks under 2050 scenarios, for which the average electricity price is $24/MWhe versus $34/MWhe in 2018. The overall pattern of operation is similar to that in Fig. 4A. The HTSE is only 4% oversized, so there is little scope to vary its output much from the average H_2 demand. The NPP reduces its output during periods when the wholesale price falls to $0.01/MWhe. This period only lasts seven hours so the NPP does not shutdown, as then it would have to wait a further 17 hours due to the 24-hour minimum shutdown constraint. The HTSE operates throughout.

The LCOH of the co-production facility is higher in 2050 than in 2018. This is because the price of electricity is lower and the NPP earns less revenue. However, the 2050 relative breakeven price of the NPP-HTSE is lower as this only considers the costs of producing H_2, which is lower as electricity is cheaper. The reduction in prices also reduces the LCOH of the independent HTSE.

Table 2. The levelized cost of hydrogen (LCOH) and relative breakeven price of hydrogen for the independent HTSE and co-production facility in each of the three scenarios. The relative breakeven price of the independent electrolyzer is equal to its LCOH as it never incurs an opportunity cost when it produces H_2.

	Electricity price timeseries year [13,24]		
	2018	2030	2050
Mean electricity price ($/MWhe)	34.30	32.00	23.85
Median electricity price ($/MWhe)	28.95	29.65	24.50
Co-production LCOH ($/kg)	4.73	4.72	5.14
Co-production Relative breakeven price: ($/kg)	2.54	2.29	1.95
Independent HTSE, no tariff LCOH ($/kg)	3.62	3.43	2.90
Independent HTSE, $10/MWh tariff LCOH ($/kg)	4.52	3.79	3.38

H_2 produced by the NPP-HTSE facility in 2030 is $0.3/kg cheaper than in 2018. While the mean price of electricity in the 2018 and 2030 scenaris is almost the same, the median price is higher, and the distribution of prices is shifted to the left and its right-hand tail is gone. This means there are more periods of low prices. By varying its output, both HTSE facilities can reduce their average price of electricity. In these runs, the effective price of electricity was as low as $10/MWh. This trend continues in 2050, where the price distribution has a bimodal peak at $0/MWh (see Fig. 3). However, the relatively high cost of H_2 storage limits the extent to which these periods of low prices can be taken advantage of.

Sensitivity to the HTSE cost and current density limit

The optimized HTSE and NPP-HTSE facilities produce expensive H_2. This is largely a function of the high cost of HTSEs and their low current density limit. We perform a sensitivity study of these values to see how they would affect the cost of H_2 and see which would be most impactful to improve.

Table 3 shows the results of the sensitivity study for the NPP-HTSE facility. As expected, increasing the current density or reducing the cost of the HTSE cause the biggest reduction in the H_2 LCOH and relative breakeven price. In both cases, it is economic to oversize the NPP-HTSE system significantly and mostly produce H_2 during periods of low prices. Fig. 5 shows an example of this for the 6A/cm^2 NPP-HTSE. The NPP exports and NPP-HTSE energy balance vary very closely with the price of electricity. As before, the NPP reduces its power output during zero-priced periods.

The other two changes had smaller impacts on the cost of H_2. Reducing the cost of the NPP reduces the LCOH of H_2 as the NPP fixed costs are less, but has no impact on the relative breakeven price as the cost of electricity is unaffected.

Table 3. The LCOH and relative breakeven price of the four sensitivity study cases. Each was evaluated using the 2050 electricity price data.

	2050 Base-case	Low-cost HTSE [16]	900C HTSE	$35 / MWh NPP [20]	6A/cm^2 HTSE
HTSE oversizing	4%	9%	1%	12%	70%
LCOH ($/kg)	5.07	3.74	4.67	2.70	3.71
Rel. break. price: ($/kg)	1.87	0.54	1.47	1.87	0.51

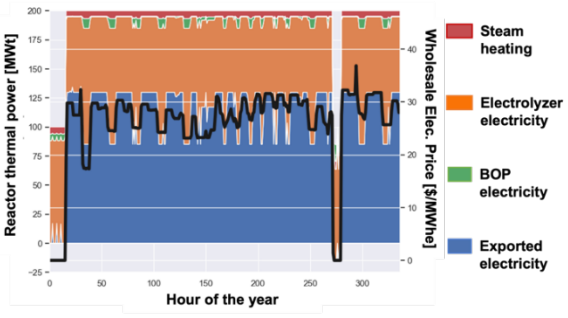

Figure 5. Dispatch and energy balance of the NPP over two weeks as part of the NPP-HTSE system for the 2050 system and a 6A/cm^2 HTSE.

CONCLUSION

In this paper we have developed an integrated design and scheduling optimization model to study grid-interactive processes producing multiple products. To solve the model, a nonconvex MINLP, we proposed a three-level decomposition approach and range of tailored approximations to identify near-optimal solutions. We then demonstrated the approach in a short case study of electricity and hydrogen co-production using a high-temperature nuclear power plant and HTSE. While there are opportunities to improve the numerical stability and runtime of the method, we have shown that it can be used to capture HTSE part load operations and high temporal resolution efficiently.

In our case study, we demonstrated the cost advantage of co-producing electricity and hydrogen using an NPP and HTSE. We have show that co-production facilities must consider the opportunity cost of not selling electricity when they price their hydrogen. We call this combination of the levelized cost of producing H_2 and the opportunity cost of not selling electricity the relative breakeven price. Through our sensitivity analysis, we highlighted how electricity prices, HTSE capital costs and current density limits, impact the minimum price of H_2

ACKNOWLEDGEMENTS

The authors acknowledge funding from Shell and feedback from Jacopo Buongiorno on the framing and approach through the course of the project.

REFERENCES

1. CRS. U.S. Nuclear Plant Shutdowns, State Interventions, and Policy Concerns (2021)
2. Sepulveda, N. A., Jenkins, J. D., de Sisternes, F. J. & Lester, R. K. The Role of Firm Low-Carbon Electricity Resources in Deep Decarbonization of Power Generation. Joule 2, 2403–2420 (2018).
3. Ruth, M. et al. The Technical and Economic Potential of the H2@Scale Concept within the United States (2020). NREL
4. Buttler, A, Spliethoff, H. Current status of water electrolysis for energy storage, grid balancing and sector coupling via power-to-gas and power-to-liquids: A review. Renewable and Sustainable Energy Reviews 82, 2440–2454 (2018).
5. Kim, J. S., Boardman, R. D. & Bragg-Sitton, S. M. Dynamic performance analysis of a high-temperature steam electrolysis plant integrated within nuclear-renewable hybrid energy systems. Applied Energy 228, 2090–2110 (2018).
6. Frick, K., Wendt, D., Talbot, P., Rabiti, C. & Boardman, R. Technoeconomic assessment of hydrogen cogeneration via high temperature steam electrolysis with a light-water reactor. Applied Energy 306, 118044 (2022).
7. Frew, B., et al. Analysis of multi-output hybrid energy systems interacting with the grid: Application of improved price-taker and price-maker approaches to nuclear-hydrogen systems. Applied Energy 329, 120184 (2023).
8. Mulder, Eben. Overview of X-Energy's 200 MWth Xe-100 Reactor, NAS (2021)
9. Dow, Dow and X-energy advance efforts, 2023
10. Orella, M. J., et al. A General Technoeconomic Model for Evaluating Emerging Electrolytic Processes. Energy Technology 8, 1900994 (2020).
11. Buttler, A., et al. detailed techno-economic analysis of heat integration in high temperature electrolysis for efficient hydrogen production. International Journal of Hydrogen Energy 40, 38–50 (2015).
12. Brents' Method. https://en.wikipedia.org/wiki/Brent%27s_method
13. National Renewable Energy Laboratory, https://www.nrel.gov/analysis/cambium.html
14. Petipas, Floriane, et al. "Thermal management of solid oxide electrolysis cell systems through air flow regulation." Chem Eng Trans 61 (2017)
15. Wendt, Daniel S., et al. High Temperature Steam Electrolysis Process Performance and Cost Estimates. No. INL/RPT-22-66117-Rev000. Idaho National Lab (2022)
16. James, Brian D., Prosser, Jacob H., Das, Sujit. HTE Stack Manufacturing Cost Analysis (2022)
17. Expert Finance Working Group. "Economic and Finance Working Group: SMR Roadmap." (2018).
18. EIA. Electric Power Monthly (2023)
19. Gurobi Optimization, LLC. Gurobi Optimizer Reference Manual (2023)
20. Mulder, Eben, et al. Advanced Operation & Maintenance Techniques Implemented in the Xe-100 Plant Digital Twin to Reduce Fixed O&M (2022)
21. Davis, Ian, Braudt, Tom, Rackiewicz, David. Xe-100 Maintenance Staffing Optimization (2021)
22. NREL. 2023 Annual Technology Baseline (2023) https://atb.nrel.gov/.
23. Houchins, Cassidy, James, Brian D. Hydrogen Storage Cost Analysis (2022)
24. MISO. Real Time Market Report (2022)